










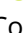







Serum and Tissue Biomarkers Associated With Composite of Relevant Endpoints for Sjögren Syndrome (CRESS) and Sjögren Tool for Assessing Response (STAR) to B Cell-Targeted Therapy in the Trial of Anti-B Cell Therapy in Patients With Primary Sjögren Syndrome (TRACTISS)

Elena Pontarini,¹  Elisabetta Sciacca,¹  Farzana Chowdhury,¹ Sofia Grigoriadou,¹ Felice Rivellese,² 
William J. Murray-Brown,¹ Davide Lucchesi,¹  Liliante Fossati-Jimack,¹  Alessandra Nerviani,²
Edyta Jaworska,¹  Giulia Maria Ghirardi,¹ Chiara Giacomassi,¹ Paul Emery,³  Wan Fai Ng,⁴  Nurhan Sutcliffe,⁵
Colin Everett,³  Catherine Fernandez,³ Anwar Tappuni,²  Raphael Seror,⁶ Xavier Mariette,⁶ Raphael Porcher,⁷
Giulia Cavallaro,⁸  Alfredo Pulvirenti,⁸  Gwenny M. Verstappen,⁹  Liseth de Wolff,⁹  Suzanne Arends,⁹
Hendrika Bootsma,⁹ Miles J. Lewis,²  Constantino Pitzalis,²  Simon J. Bowman,¹⁰
and Michele Bombardieri,²  on behalf of the Trial for Anti-B Cell Therapy in Patients With Primary Sjögren Syndrome Study Research Group

Objective. This study aimed to identify peripheral and salivary gland (SG) biomarkers of response/resistance to B cell depletion based on the novel concise Composite of Relevant Endpoints for Sjögren Syndrome (cCRESS) and candidate Sjögren Tool for Assessing Response (STAR) composite endpoints.

Methods. Longitudinal analysis of peripheral blood and SG biopsies was performed pre- and post-treatment from the Trial of Anti-B Cell Therapy in Patients With Primary Sjögren Syndrome (TRACTISS) combining flow cytometry immunophenotyping, serum cytokines, and SG bulk RNA sequencing.

Results. Rituximab treatment prevented the worsening of SG inflammation observed in the placebo arm, by inhibiting the accumulation of class-switched memory B cells within the SG. Furthermore, rituximab significantly down-regulated genes involved in immune-cell recruitment, lymphoid organization alongside antigen presentation, and T cell costimulatory pathways. In the peripheral compartment, rituximab down-regulated immunoglobulins and auto-antibodies together with pro-inflammatory cytokines and chemokines. Interestingly, patients classified as responders according to STAR displayed significantly higher baseline levels of C-X-C motif chemokine ligand-13 (CXCL13), interleukin (IL)-22, IL-17A, IL-17F, and tumor necrosis factor- α (TNF- α), whereas a longitudinal analysis of serum T cell-related cytokines showed a selective reduction in both STAR and cCRESS responder patients. Conversely, cCRESS response was better associated with biomarkers of SG immunopathology, with cCRESS-responders showing a significant decrease in SG B cell infiltration and reduced expression of transcriptional gene modules related to T cell costimulation, complement activation, and Fc γ -receptor engagement. Finally, cCRESS and STAR response were associated with a significant improvement in SG exocrine function linked to transcriptional evidence of SG epithelial and metabolic restoration.

Conclusion. Rituximab modulates both peripheral and SG inflammation, preventing the deterioration of exocrine function with functional and metabolic restoration of the glandular epithelium. Response assessed by newly developed cCRESS and STAR criteria was associated with differential modulation of peripheral and SG biomarkers, emerging as novel tools for patient stratification.

The views expressed herein are those of the authors and do not necessarily represent those of the National Institute for Health Research (NIHR) or the Department of Health and Social Care.

Supported by Versus Arthritis UK (grants 21-753 and 20-089 to Drs. Pontarini and Bombardieri, respectively), the William Harvey Research

Foundation (to Dr. Bombardieri), Medical Research Council (grants MRC MR/T016736/1 and MR/N003063/1 to Dr. Bombardieri), and Foreum (Stratified medicine in Sjögren syndrome to Dr. Ng). Also supported by the NIHR Barts Biomedical Research Centre (grant NIHR203330 to Drs. Pitzalis and Bombardieri). This project was also supported by the Innovative

INTRODUCTION

Primary Sjögren syndrome (pSS) is a systemic autoimmune disease characterized by chronic inflammation of the exocrine glands, mainly the salivary and lacrimal glands, leading to impaired secretory function and sicca symptoms. Most patients report fatigue and pain, and approximately 30% to 50% of patients develop systemic manifestations.¹ Currently, the treatment of pSS is mainly symptomatic with tears and saliva substitutes, saliva-stimulating agents, and analgesics, together with systemic corticosteroids and immunosuppressants for patients with systemic involvement. However, the efficacy of these treatments is modest, and a proper disease-modifying treatment aiming at reducing disease activity is missing.²

The pathogenic role of B cells in pSS is well established, and B cell abnormalities are hallmarks of the disease, resulting in the presence of circulating autoantibodies, peripheral B cell subset alterations,^{3,4} and B cell predominance in advanced salivary gland (SG) lesions with organization of ectopic germinal centers (GCs) in approximately 30% to 40% of patients.⁵ B cell hyperactivity in pSS also leads to an increased risk of developing non-Hodgkin B cell lymphomas.⁶

Despite the well-recognized role of B cells in pSS pathogenesis, the beneficial role of B cell depletion therapy with rituximab, a chimeric anti-CD20 (a B cell-specific membrane protein) monoclonal antibody, remains elusive. Several single-arm, open-label, and randomized controlled trials (RCTs) evaluated the efficacy of rituximab in pSS, showing an improvement in pSS symptoms, such as fatigue, dryness, and pain but also of systemic inflammatory manifestations. Following on from early, small-scale studies showing promising results,⁷ two large RCTs, Tolerance and Efficacy of Rituximab in Primary Sjögren's Syndrome (TEARS)⁸ and Trial of Anti-B Cell Therapy in Patients With pSS (TRACTISS),⁹ administering one and two cycles of rituximab, respectively, did not meet their primary endpoints, indicating either lack of efficacy or low sensitivity to change of the primary endpoint. Of note, the reanalysis of both the TEARS and TRACTISS trials, based on the

recently developed Composite of Relevant Endpoints for Sjögren Syndrome (CRESS)¹⁰ and Sjögren Tool for Assessing Response (STAR)¹¹, demonstrated a significantly higher response rate in patients who received rituximab compared to placebo arm. This prompted an analysis of peripheral compartment, histopathology, and SG transcriptomic signatures to identify biomarkers of response/resistance. To date, the TRACTISS is the largest multicenter, placebo-controlled, phase III trial investigating the impact of two cycles of receiving rituximab (or placebo) at baseline and 24 weeks, with a follow-up at 48 weeks.¹² Despite the unmet primary endpoints (>30% reduction in fatigue or oral dryness measured by visual analog scale [VAS]), patients who received rituximab showed an improvement in secondary endpoints, like unstimulated whole salivary flow (UWSF),⁹ and SG total ultrasound (US) score.^{10,11,13} The higher response rates reported for concise CRESS (cCRESS) and candidate STAR scores in the patients who received rituximab are driven by the improvement in clinical EULAR Sjögren Syndrome Disease Activity Index (ESSDAI) and UWSF, alongside a reduction of serum rheumatoid factor (RF) and immunoglobulin-G (IgG) level.^{10,11}

Overall, these subanalyses suggested that rituximab could help to preserve the exocrine function of SGs if administered when a residual glandular function is still present. However, the impact of rituximab on SG inflammation is still unclear because it has only been explored in small observational studies, with conflicting results possibly caused by the differences in the study design, disease stage, and the degree of SG inflammation but also different timing in the assessment of post-treatment SG biopsies. In addition, peripheral/histologic biomarkers of response/resistance are still lacking to enable patients' stratification. Here, we present the peripheral, histologic, and transcriptomic analysis of longitudinal matched blood and labial SG (LSG) biopsies in the pSS cohort receiving rituximab or placebo within the TRACTISS trial, according to treatment response re-evaluated using the cCRESS and STAR composite endpoints.

Medicines Initiative 2 Joint Undertaking (JU) NECESSITY (grant 806975). The JU receives support from the European Union's Horizon 2020 research and innovation program and the European Federation of Pharmaceutical Industries and Associations. The present article reflects only the authors' views, and the JU is not responsible for any use that may be made of the information it contains. Dr. Rivellese work was supported by an NIHR Transitional Research Fellowship (grant TRF-2018-11-ST2-002). Dr. Bowman's work was supported by the NIHR Birmingham Biomedical Research Centre and the NIHR/Wellcome Trust Birmingham Clinical Research Facility.

¹Elena Pontarini, PhD, Elisabetta Sciacca, PhD, Farzana Chowdhury, PhD, Sofia Grigoriadou, PhD, William J. Murray-Brown, PhD, Davide Luchessi, PhD, Liliane Fossati-Jimack, PhD, Edyta Jaworska, MSc, Giulia Maria Ghiardi, MSc, Chiara Giacomassi, PhD: Queen Mary University of London, London, UK; ²Felice Rivellese, PhD, Alessandra Nerviani, PhD, Anwar Tappuni, PhD, Miles Lewis, PhD, Constantino Pitzalis, PhD, Michele Bombardieri, PhD: Queen Mary University of London and Bart's Health NHS Trust, London, UK; ³Paul Emery, MD, Colin Everett, PhD, Catherine Fernandez, PhD: University of Leeds, Leeds, UK; ⁴Wan-Fai Ng, PhD: Newcastle University and NIHR Newcastle Clinical Research Facility, Newcastle upon Tyne, UK; ⁵Nurhan Sutcliffe, MD: Bart's Health NHS Trust, London, UK; ⁶Raphael Seror, PhD, Xavier

Mariette, PhD: Université Paris-Saclay, and AP-HP, Hôpital Bicêtre, Le Kremlin-Bicêtre, France; ⁷Raphael Porcher, PhD: Université Paris Cité, Centre de Recherche Épidémiologie et Statistiques Paris, France; ⁸Giulia Cavallaro, MSc, Alfredo Pulvirenti, PhD: University of Catania, Catania, Italy; ⁹Gweny Verstappen, PhD, Liseth de Wolff, PhD, Suzanne Arends, PhD, Hendrika Bootsma, PhD: University Medical Center Groningen, University of Groningen, Groningen, The Netherlands; ¹⁰Simon J. Bowman, PhD: University Hospitals Birmingham NHS Foundation Trust, Birmingham, UK.

Drs. Pontarini, Sciacca, and Chowdhury contributed equally to this work.

Additional supplementary information cited in this article can be found online in the Supporting Information section (<http://onlinelibrary.wiley.com/doi/10.1002/art.42772>).

Author disclosures and graphical abstract are available at <https://onlinelibrary.wiley.com/doi/10.1002/art.42772>.

Address correspondence via email to Michele Bombardieri, PhD, at m.bombardieri@qmul.ac.uk or to Elena Pontarini, PhD, at e.pontarini@qmul.ac.uk.

Submitted for publication July 7, 2023; accepted in revised form December 4, 2023.

PATIENTS AND METHODS

Study cohort and sample collection. The TRACTISS study was approved by Leeds Research Ethics Committee (reference 10/H1307/99). Patients received either two doses, two weeks apart, of intravenous rituximab (1,000 mg) or placebo (250 mL saline) in two courses at weeks 0 and 2, 24, and 26 in combination with corticosteroid in both arms.¹² Demographic, clinical, and laboratory parameters of the whole pSS cohort ($n = 133$)⁹ in comparison with the SG biopsy cohort ($n = 29$) are shown in Supplementary Tables 1 and 2. Patients provided written informed consent for LSG biopsies at weeks 0, 16, and 48. Treatment response at 48 weeks was assessed using the cRESS¹⁰ and candidate STAR¹¹ composite scores and the ESSDAI improvement from baseline.

LSG biopsies histology. The histology protocol is detailed in Supplementary Methods. All primary and secondary antibodies are listed in Supplementary Table 3. Whole slide images were acquired with Hamamatsu NanoZoomerS60 Slide Scanner. Based on B cell, T cell, and follicular dendritic cell (FDC) staining, inflammatory infiltrate organization was scored using semiquantitative grading by two independent operators.

Digital imaging analysis for histologic assessment. The digital imaging analysis was performed using QuPath open source software (version 2.0-m9).^{14,15} For each sample, more than one lobule was analyzed to achieve the recommended minimum glandular area of 8 mm².¹⁶ On hematoxylin and eosin (H&E) images, the foci (≥ 50 periductal mononuclear cells) were enumerated manually, whereas total SG and aggregate areas were digitally measured. The focus score and the aggregate (foci) area fractions were calculated as follows:

$$\text{Focus score} = [\text{infiltrate number} \times 4] / \text{total SG area (mm}^2\text{)}$$

$$\begin{aligned} \text{Aggregate area fraction (\%)} \\ = [\text{aggregate area (mm}^2\text{)} \times 100] / \text{total SG area (mm}^2\text{)} \end{aligned}$$

For immunofluorescence stainings (CD20, CD3, and CD138), the total SG area and area and count of positive cells were digitally quantified to calculate the positive cell area fraction and positive cell density as follows:

$$\begin{aligned} \text{Positive cell area fraction (\%)} \\ = [\text{positive cell area (mm}^2\text{)} \times 100] / \text{total SG area (mm}^2\text{)} \end{aligned}$$

$$\begin{aligned} \text{Positive cell density (cell number/mm}^2\text{)} \\ = \text{positive cell number} / \text{total SG area (mm}^2\text{)} \end{aligned}$$

RNA extraction and bulk messenger RNA sequencing of LSG biopsies. One LSG lobule per patient was stored in RNAlater solution for 24 hours at 4°C and transferred at -80°C for long-term storage. SG RNA was extracted using RNeasy Micro Kit (Qiagen) as per the manufacturer's instructions, quantified and checked for integrity using Qubit-2.0 Fluorometer (Invitrogen) and TapeStation (Agilent Technologies), respectively. Total RNA (500 ng) was outsourced for the sequencing of bulk messenger-RNA (mRNA). Bulk mRNA sequencing of LSG biopsies and transcriptomic analysis are detailed in Supplementary Methods.

Flow cytometry and cytokines detection. Flow cytometry and cytokines detection Flow cytometry on peripheral blood mononuclear cells and cytokine detection in serum are described in Supplementary Methods.

Statistical analysis. Differences in quantitative variables between two groups were analyzed by Mann-Whitney two-tailed U-test or independent samples *t*-test as appropriate after assessing the data distribution using Shapiro-Wilk normality test. For multiple comparisons, Kruskal-Wallis test with Dunn's post hoc correction or two-way analysis of variance (ANOVA) was used. Wilcoxon's rank sum test was used for paired analysis. The χ^2 test with Yates's correction or Fisher's exact test, as appropriate, was used in the contingency table analysis. Spearman's rank analysis was performed for non-parametric variable correlations. *P* values less than 0.05 were considered significant. Statistical analyses were performed using GraphPad Prism 9.0.

Data sharing statement. The SG RNA-sequencing (RNA-seq) data, including longitudinal expression of individual genes and their transcript level according to histology, clinical parameters, and clinical response, in pSS patients recruited in the TRACTISS trial, are publicly available at the interactive web interface <https://tractiss.hpc.qmul.ac.uk/>

RESULTS

Correlation of clinical, histologic, and biologic parameters. As part of the TRACTISS sub-analysis, clinical, serological, and histologic analyses were performed on matched blood and lip biopsy samples collected according to Figure 1A. First, we looked at correlations among clinical, immunologic, and histopathological features at baseline (Figure 1B). Objective measurements of secretory function, such as unstimulated and stimulated salivary flow and Schirmer's test, but also foci average area, showed the strongest correlation with patient's dryness assessed on a VAS. Of note, Schirmer's test showed an inverse correlation with SG US and circulating RF. SG histologic measurements, such as focus score, foci area, B and T cell density, and area fraction but also B cell aggregates counts, had significant correlations

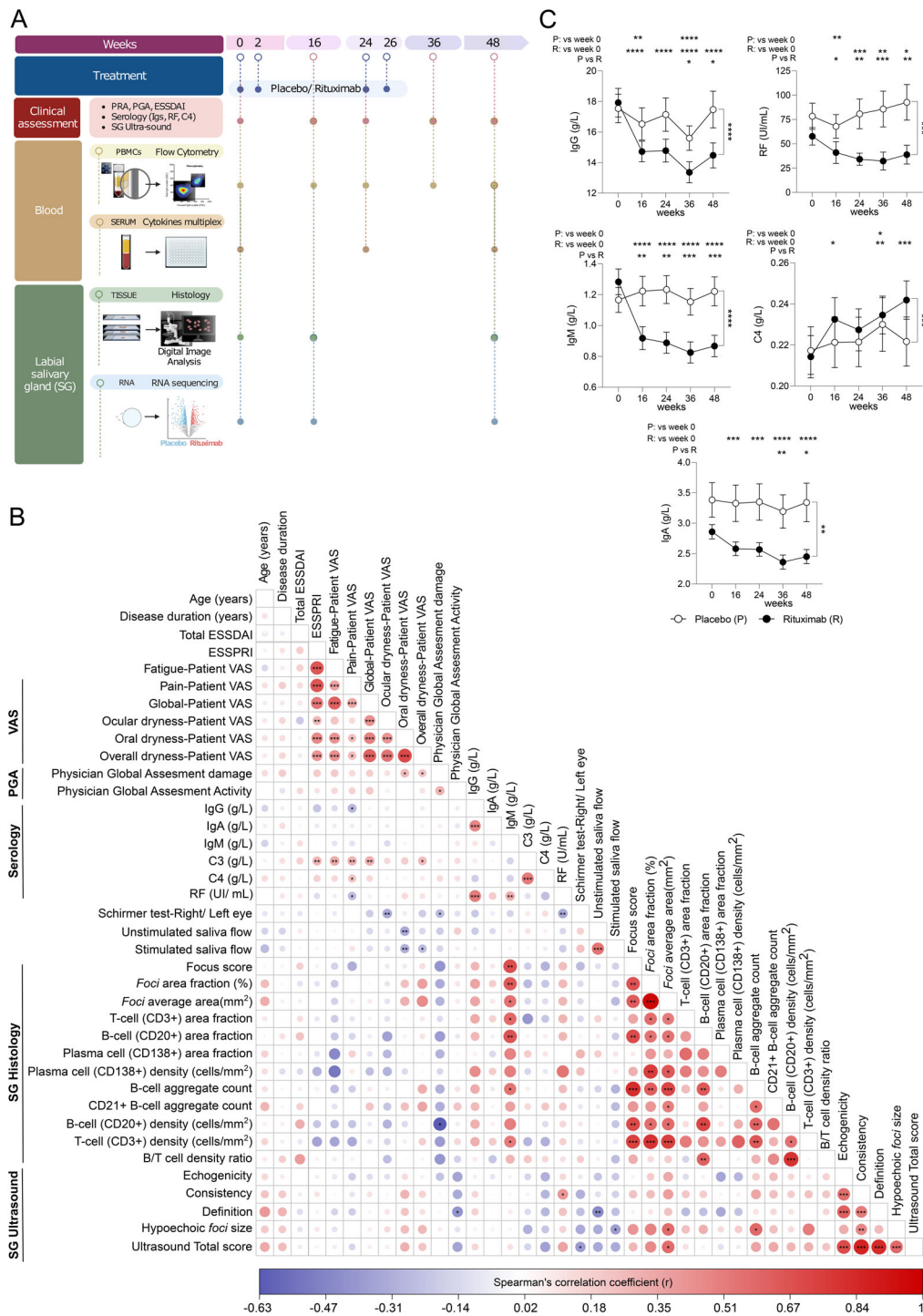


Figure 1. Correlogram of baseline clinical, immunologic, and histopathological variables in the TRACTISS cohort. (A) The TRACTISS sub-analysis of peripheral blood and LSG biopsies. (B) Correlation matrix of baseline clinical, serologic, and histologic variables of TRACTISS cohort (n = 133). Histology is available for a subset of patients (n = 29). The size of the circle encodes for the magnitude of each correlation, whereas the color of the dot denotes the value of the Spearman correlation coefficient (r). The P values are adjusted for multiple testing with false discovery rate correction and are shown within the dots when statistically significant. *P < 0.05, **P < 0.01, ***P < 0.001. (C) Changes overtime (weeks 0, 16, 24, 36, and 48) in circulating Igs (IgG, IgM, and IgA), RF, and complement C4 in the group that received placebo (n = 63) and the group that received rituximab (n = 62). Mean ± SEM values are shown. Wilcoxon's rank sum test was performed within groups and Mann-Whitney U test between groups. Two-way analysis of variance mixed model (time:treatment ratio) appears on side square brackets. *P < 0.05, **P < 0.01, ***P < 0.001, ****P < 0.0001. ESSDAI, EULAR Sjögren's syndrome disease activity index; ESSPRI, EULAR Sjögren's Syndrome Patient Reported Index; PBMC, peripheral blood mononuclear cell; PGA, physician global assessment; PRA, patient reported assessment; RF, rheumatoid factor; SG, salivary gland; TRACTISS, Trial for Anti-B Cell Therapy in Patients With Primary Sjögren Syndrome; VAS, visual analog scale.

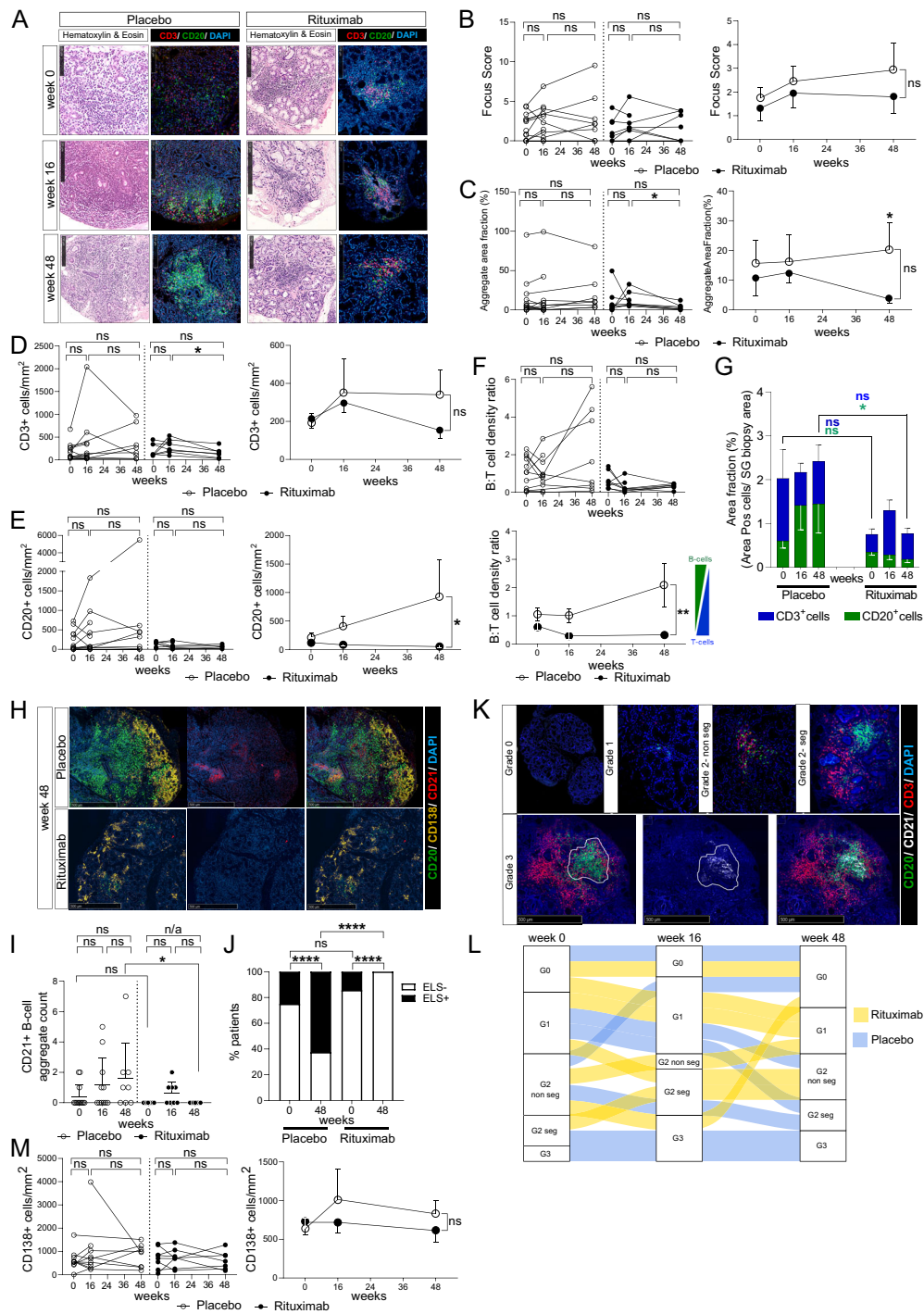


Figure 2. Rituximab prevents glandular B cell infiltration and ELS development. (A) Representative images of LSGs for focus score assessment and B (CD20⁺) and T (CD3⁺) cell quantification. (B) Changes overtime in focus score, (C) aggregate area fraction, (D and E) T and B cell density, (F) B/T cell density ratio, and (G) T (blue) and B cell (green) area fraction. ns $P \geq 0.05$, * $P < 0.05$, ** $P < 0.01$. (H) Representative image of ectopic germinal center organization with CD21⁺ FDC network within B cell aggregate, with peri-aggregate CD138⁺ plasma cells at week 48. Changes overtime in the (I) number of B cell aggregates with FDC networks and (J) the ELS prevalence. ns $P \geq 0.05$, * $P < 0.05$, **** $P < 0.0001$. (K) Representative images depicting semiquantitative grading for aggregate organization. For grade 3, B cell aggregate is outlined (bottom, left), within which the FDC network forms (bottom, middle), overlaid in right, bottom panel. Changes overtime in the (L) semiquantitative grading (one line per patient) and (M) plasma cell density. Data from patients who received placebo (n = 12) and patients who received rituximab (n = 8). ns $P \geq 0.05$. (B–F and M) Individual patient data are shown on left graph (Wilcoxon’s rank sum test within groups) and mean \pm SEM of the groups that received placebo and rituximab on the right graph. Two-way analysis of variance mixed model (time:treatment ratio) appears on side square brackets. ELS, ectopic lymphoid structure; FDC, follicular dendritic cell; n/a, not available; non Seg, non segregated; seg, segregated; ns, not significant; . Color figure can be viewed in the online issue, which is available at <http://onlinelibrary.wiley.com/doi/10.1002/art.42772/abstract>.

with serum IgM levels. Similarly, IgM and IgG serum levels showed the strongest positive correlations with RF. Among the histologic parameters, the foci average area and area fraction were the only histologic parameters positively correlating with the US total score (Figure 1B; Supplementary Figure 1A). When assessing the longitudinal effect of rituximab, Igs (IgA, IgG, and IgM) and RF were significantly reduced alongside an increment of C4 compared to placebo (Figure 1C).

Rituximab prevents SG B cell infiltration and ectopic GC organization. LSG biopsies, collected at weeks 0, 16, and 48 (Figure 1A), were stained for H&E (Figure 2A) to quantify the degree of LSG inflammation. There was no difference in the focus score between patients who received placebo and those who received rituximab at week 48 or a change in focus scores between week 0 and 16 or 48 within each group (Figure 2B). However, because the focus score only assesses the number of inflammatory infiltrates/area without discriminating the size of the aggregates, a quantitative assessment of aggregates was performed, measuring their average absolute size and area relative to the total gland area (area fraction). The LSGs of patients who received rituximab showed significantly smaller aggregates and lower foci area fraction at week 48 compared to the LSGs of patients who received placebo (Figure 2C; Supplementary Figure 1B).

The effect of rituximab on aggregate size is likely explained by its impact on B cell infiltration. Accordingly, patients who received rituximab had significantly lower B cell density and B cell area fraction (Figure 2E and G) at 48 weeks. More specifically, rituximab seemed to prevent the increase in B cell infiltration observed in the placebo group by week 48, despite the peripheral repopulation occurring after week 16 (Supplementary Figure 1C). In contrast, T cells showed no difference between the group who received rituximab and the placebo group, both in terms of area fraction and cell density (Figure 2D and G). The effects on B cell infiltration were confirmed on a second cutting level (Supplementary Figure 1D) and by the B/T cell density ratio, which was reduced in the rituximab arm by week 48 (Figure 2F).

By preventing the increase of SG B cell infiltration, rituximab also prevented the development of FDC networks within B cell aggregate (Figure 1H). Lower count of B cell aggregate positive for CD21⁺ FDC and a lower prevalence of ectopic lymphoid structures (ELs) were observed in patients who received rituximab, compared to placebo by week 48 (Figure 2I and J). Although ELs are known to be local niches for maturation/differentiation of autoreactive B and plasma cells, to date, there are no data portraying their evolution over time in the SGs of patients with pSS. In this cohort, the assessment of ELs in serial LSG biopsies revealed a worsening of aggregate organization in patients who received placebo compared to rituximab. Small aggregates at baseline (G0, G1, and G2 non-segregated) tended to change toward larger diffuse foci with clear B/T cell segregation

(G2 segregated) and presence of FDC networks (G3), features of ELs, in patients who received placebo by week 48 (Figure 2K and L). On the other hand, no difference was observed in plasma cells surrounding the inflammatory aggregates (Figure 2M).

Two rituximab cycles prevent the progression of SG inflammation. To further explore the effects of rituximab versus placebo on LSGs, we performed bulk RNA-seq and applied cellular deconvolution methods. Considering the variety of transcriptome-based, cell-type quantification methods,¹⁷ both deconvolution and marker gene-based methods were first compared and validated against histopathology (Supplementary Figure 2A and B). xCell,¹⁸ a gene signature-based deconvolution tool identifying 35 immune-cell signatures, was selected because it showed the best correlations with histopathology in our dataset (Supplementary Figure 2A and B). At week 48, LSGs of placebo patients showed an enrichment of immune cells, such as B cells, CD4⁺ and CD8⁺ T cells, and dendritic cell (DC) subsets compared to baseline, indicating an evolution/worsening of SG immunopathology over time (Figure 3A). In contrast, receiving rituximab decreased and/or prevented further enrichment of immune cells within LSGs, except for the myeloid compartment (Figure 3B).

To differentiate the effects of the first and second cycles of rituximab on the immune cell subsets, the delta change (Δ) variation in the xCell enrichment scores between baseline and week 16 or 48 (Δ for week 48 [$\Delta 48$]) was calculated. As expected, receiving rituximab affected the B cell compartment, in particular, memory B cells (class-switched memory B cells) or DCs (Figure 3C and D; Supplementary Figure 2C). However, a significant reduction in the memory B cells was only observed after the second cycle ($\Delta 48$) (Figure 3C and D). Consistent with our histologic data, T cell subsets (naive, central memory, effector memory, T helper-1, T helper-2, and T regulatory) did not show significant changes over time (Supplementary Figure 2D).

When looking at the changes in individual gene expression over time, rituximab reduced the expression of several genes linked to ectopic GC organization and functionality (Figure 3E–G), like CD19, interleukin (IL)-21, IL-21 receptor, and C-X-C motif chemokine ligand (CXCL) 13, and cell subsets driving follicular and extrafollicular response in the SGs of patients with pSS. Accordingly, T follicular and T peripheral helper cell¹⁹ modules were reduced after the second infusion of rituximab (Figure 3H).

Accordingly, modular analysis based on co-expressed genes^{20,21} showed how rituximab treatment down-regulated modules associated with immune response initiation, complement-dependent and antibody-mediated cytotoxicity (known mechanisms of rituximab action initiated by Fc γ receptor engagement, module 11), T cell costimulation, and interferon- γ (module 7) signaling (Supplementary Figure 3A and B) by week 48. Of note, modules associated with SG restoration, such as retinoid metabolism (module 13) involved in SG morphogenesis,²² were

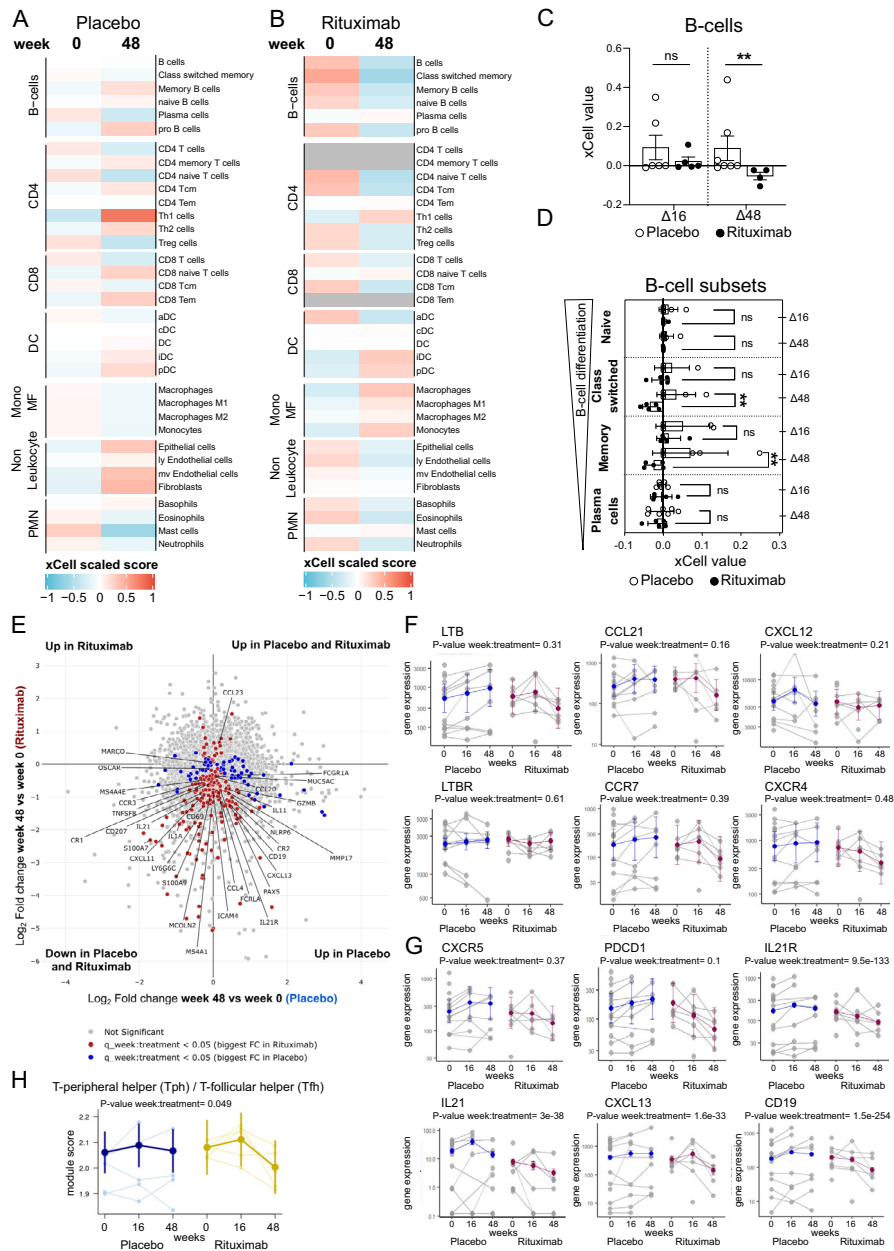


Figure 3. Rituximab prevents the glandular infiltration of memory B cells and the expression of ectopic germinal center-related genes. Heatmaps with xCell average score for each cell type at weeks 0 and 48, in the LSG of (A) patients who received placebo and (B) patients who received rituximab. xCell score delta change for (C) B cells and (D) B cell subsets between week 16 ($\Delta 16$) and week 48 ($\Delta 48$). Mann–Whitney U test was used. $Ns P \geq 0.05$, $**P < 0.01$. (E) Scatter plots comparing longitudinal gene expression changes between weeks 48 and 0 in patients who received placebo and those who received rituximab, on the x and y axis, respectively. Genes with greater absolute fold change following patients receiving rituximab or placebo are shown in red and blue, respectively. (F) Changes over time in the expression of genes involved in the ectopic lymphoid structure organization and (G) germinal center reaction. Blue (placebo) and red (rituximab) lines represent the negative binomial mixed-effects model fitted for each gene with 95% confidence interval for the fixed effects. (H) Changes in the Tph and Tfh cell modules over time. Blue (placebo) and yellow (rituximab) lines represent the normal mixed-effects model fitted for Tph and Tfh cell module scores. The P values of the week:treatment ratio interaction model are shown on top. Data from patients who received placebo ($n = 12$) and patients who received rituximab ($n = 8$) are shown. $\Delta 16$, delta change for week 16-0; $\Delta 48$, delta change for week 48-0; aDC, activated dendritic cell; CCR, C-C motif chemokine receptor; DC, dendritic cell; cDC, conventional DC; CR, complement receptor; CXCL, C-X-C motif chemokine ligand; CXCR, C-X-C motif chemokine receptor; FCGR, Fc receptor-like; FCRL, Fc receptor-like; GZM, Granzyme; ICAM, intercellular adhesion molecule; iDC, immature DC; IL, interleukin; Iy, lymphatic; LTB, lymphotoxin-B; LTBR, LTB receptor; MARCO, macrophage receptor with collagenous structure; MCOLN, mucopolipin cation channel; MF, macrophage; MMP, matrix metalloproteinase; Mono, monocyte; MUC, mucin; mv, micro vascular; ns, not significant; OSCAR, osteoclast-associated Ig-like receptor; pDC, plasmacytoid DC; PDCD, programmed cell death; PMN, polymorphonuclear cell; Tcm, T central memory; Tem, T effector memory; Tfh, T follicular helper; Th, T helper; TNFSF, tumor necrosis factor superfamily; Tph, T peripheral helper; Treg, T regulatory. Color figure can be viewed in the online issue, which is available at <http://onlinelibrary.wiley.com/doi/10.1002/art.42772/abstract>.

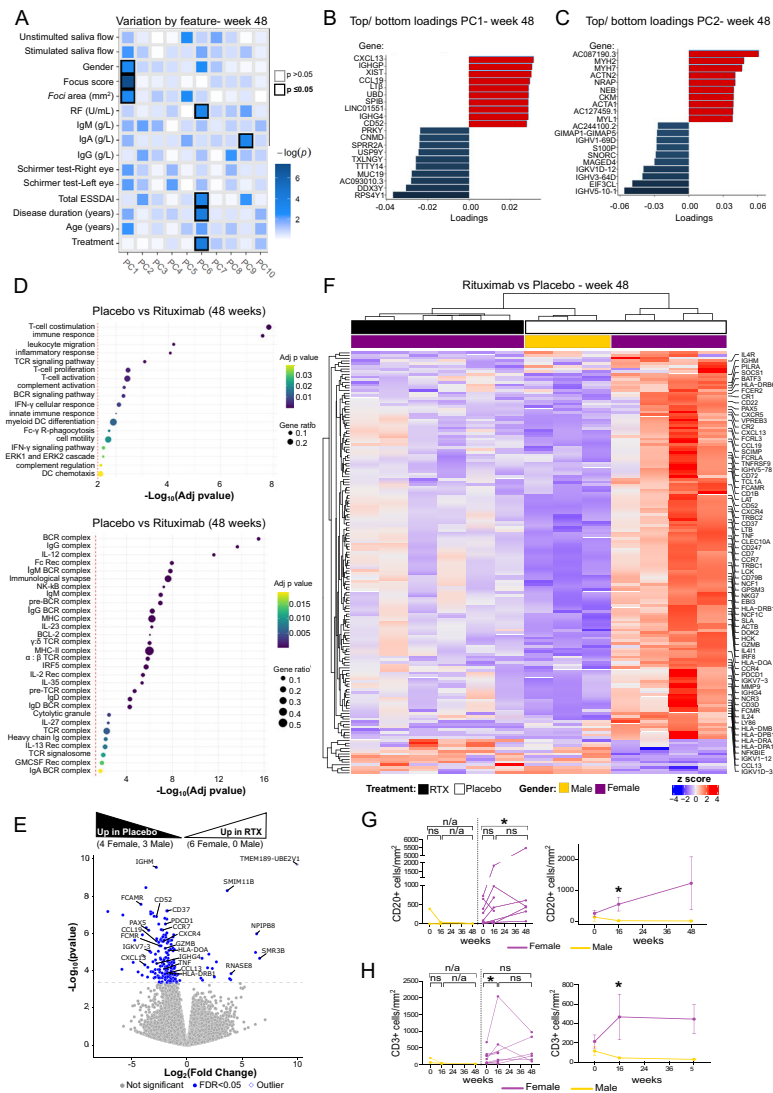


Figure 4. Differential evolution in transcriptomic and histologic changes in labial salivary gland biopsies driven by sex. (A) Tile plot depicts the correlation among the top 10 PCs of transcriptomic data and clinical variables at week 48. Black outlined tiles show significant correlations. The loading plots identify genes that have the largest effect on (B) PC1 and (C) PC2. Loadings close to -1 or 1 and close to 0 indicate, respectively, genes with strong and weak influence on the component. (D) Gene Ontology pathways associated with DEGs down-regulated in patients who received rituximab versus those who received placebo at week 48. The dashed line represents adjusted $P = 0.05$. Dot sizes are proportional to the ratio between the number of genes found as DEGs and those included in the pathway. (E) Volcano plot showing DEGs between patients who received placebo and those who received rituximab at week 48. Blue dots represent genes with $q < 0.05$. (F) Supervised clustering of normalized DEGs between patients who received rituximab and placebo at week 48. Longitudinal histologic assessment of (G) B cell and (H) T cell density in LSG biopsies of male (yellow) and female (purple) patients who received placebo. Wilcoxon's rank sum test was used within groups and Mann-Whitney U test between groups. Data are shown from the LSG biopsies of patients who received placebo ($n = 7$) and rituximab ($n = 6$). $*P < 0.05$, ns $P \geq 0.05$. ACTA; ACTB; ACTN; Adj, adjusted; BATF; BCL; BCR, B cell receptor; CCR; CKM; CLEC; CNMD; CR, complement receptor; CXCL, C-X-C motif chemokine ligand; CXCR, C-X-C motif chemokine receptor; DC, dendritic cell; DDX, DEAD box; DEG, differentially expressed gene; DMB, dimethylene blue; DOA; DOK; DPA, dual-photon absorptiometry; DRA; DRB, 5,6-dichlorobenzimidazole riboside; EBI, Epstein-Barr virus-induced gene; EIF, eukaryotic initiation factor; ESSDAI, EULAR Sjögren Syndrome Disease Activity Index; FcγR, Fcγ receptor; FCAMR; FCMR; FCER; FCRL, Fc receptor-like; FDR, false discovery rate; GIMAP; GMCSF; GPSM; GZMB; HCK; IFN, interferon; IGHG; IGHGP; IGHM; IGHV; IGKV; IRF, IFN regulatory factor; LCK, lymphocyte-specific kinase; LINC; LT, lymphotoxin; LTB, lymphotoxin-B; MHC, major histocompatibility complex; MMP, matrix metalloproteinase; MUC, mucin; MYH; MYL; n/a, not available; NCF, neutrophil cytosolic factor; NCR, noncoding region; NKG, natural killer cell receptor group; NK-kB; NPIP; NRAP, nebulin-related-anchoring protein; ns, not significant; PC, principal component; PDCD, pyruvate dehydrogenase complex deficiency; PILRA; PRKY; Rec, receptor; RPS, ribosomal protein; RTX, rituximab; SCIMP; SLA, soluble liver antigen; SMIM; SMR; SOCS, suppressor of cytokine signaling; SPIB; SPRR; TCL; TCR, T cell Rec; TMEM; TNF, tumor necrosis factor; TNFRSF, TNF Rec superfamily; TRBC; TTTY; TXLNGY; UBD; UBE; USP, ubiquitin-specific protease; VPRES; XIST. Color figure can be viewed in the online issue, which is available at <http://onlinelibrary.wiley.com/doi/10.1002/art.42772/abstract>.

up-regulated after two rituximab infusions (Supplementary Figure 3C).

Principal component analysis identifies the main factors influencing SG inflammation over time. Principal component (PC) analysis was applied to LSG transcriptomic data at weeks 0, 16, and 48, followed by linear regression analysis to correlate demographic and clinical features to the top 10 PCs responsible for observed variations between rituximab and placebo groups. Surprisingly, in addition to SG focus score and the foci area fraction, sex appeared as a key influencer of the PC1, responsible for 25.6% of the variation between placebo and rituximab patients at week 48 (Figure 4A). Of note, foci area and IgM serum level significantly correlate to PC1 at baseline, similar to focus score and IgG level at week 16 (Supplementary Figure 4A–D). Inspection of the loadings scores for the first two PCs showed chemokine ligand genes regulating B and T cell trafficking, such as CXCL13 and CCL19, and lymphoid organization genes like lymphotoxin- β among the top 10 genes that mostly influence PC1 and PC2 at week 48 (Figure 4B and C).

Analysis of differentially expressed genes (DEGs) at week 48 demonstrated down-regulation of genes and pathways linked to immune-cell activation and ectopic GC organization in rituximab patients compared to placebo (Figure 4D–F). Pathway analyses showed an increase of several B and T cell pathways in placebo arm compared to rituximab, including leukocyte migration, T cell costimulation pathways, DC chemotaxis, major histocompatibility complex class II antigen presentation, B cell receptor and Ig receptor, and CD40 receptor complex pathways (Figure 4D; Supplementary Figure 4E).

Of note, the heatmap with DEGs at week 48 highlighted a clear segregation of the placebo patients in two clusters matching with sex. LSGs of female patients with pSS showed a selective up-regulation of inflammatory genes (Figure 4F; Supplementary Figure 4F). Looking at the LSG inflammation progression in the patients who received placebo, segregated by sex, only female patients showed a higher T cell (CD3⁺) density by week 16, with an increase in B cell infiltration (CD20⁺) by week 48 (Figure 4G and H). Overall, this indicates that female patients with pSS display worse SG inflammation progression over time compared to male counterparts.

Longitudinal changes in SG histology and transcriptomic modules in association with treatment response. When patients who received rituximab were stratified by response, patients who responded to cCRESS showed a significant reduction in SG B cell infiltration (reflecting a similar trend in the aggregate area fraction and size; Supplementary Figure 5) over time by week 48 (Figure 5A), compared to patients who did not respond to cCRESS, despite the peripheral B cell depletion (Figure 5B) occurring in both patients who did and did not

respond. Similar results were not confirmed in patients who responded to STAR (Supplementary Figure 6A), suggesting that cCRESS may better mirror glandular activity by giving equal weight to the glandular versus systemic domains. Next, we applied modular analysis to identify clinically relevant molecular pathways associated with the treatment response (Figure 5C). In keeping with the B cell histology data, patients who responded to cCRESS showed a significant down-regulation of molecular pathways associated with SG immunopathology, including complement activation, Fc receptor engagement and T cell activation (modules 3, 8, and 11; Figure 5D). In parallel, patients who responded to cCRESS also showed a progressive improvement in UWSF (Figure 5F), mirrored by the up-regulation of molecular pathways indicative of functional and metabolic restoration of the glandular epithelium (modules 5, 9, and 14; Figure 5E), with similar results for patients who responded to STAR (Figure 5G; Supplementary Figure 6B). Total list of genes for each module for the Cemitool analysis and the associated pathways are present in Supplementary Tables 4 and 5. Because of the lack of biopsies from male patients in the group who received rituximab, we could not assess the influence of sex on treatment response.

Identification of peripheral biomarkers associated with SG inflammation and clinical response to receiving rituximab.

To identify predictors of treatment response, the baseline histologic and peripheral blood parameters were segregated according to response criteria defined using either ESSDAI minimal clinical improvement (MCI), cCRESS, or candidate STAR score. Analysis of baseline histology or routine blood parameters (Igs, RF, and complement) did not identify any predictors of treatment response (Supplementary Figure 7). Baseline circulating B cell frequency was also not associated with clinical response, but higher repopulation rates at week 24 occurred in patients who responded according to ESSDAI (Supplementary Figure 8A).

When comparing baseline serum cytokines levels involved in T and B cell responses, we observed significantly higher baseline levels of peripheral CXCL13, IL-22, IL-17A, IL-17F, and tumor necrosis factor (TNF)- α in patients classified as responders according to STAR, but not cCRESS, response criteria (Figure 6A–C), but not in SGs (Supplementary Figure 8B–D). The cytokine pattern in the STAR-responder patients was similar to the patients with an ESSDAI MCI of 3 points (Figure 6C and D), suggesting that patients who were more immunologically active systemically were more amenable to immunomodulation with rituximab. Accordingly, longitudinal analysis of serum cytokines confirmed a reduction in cytokine levels from baseline only in rituximab responders patients according to STAR and/or cCRESS (Figure 6E and F).

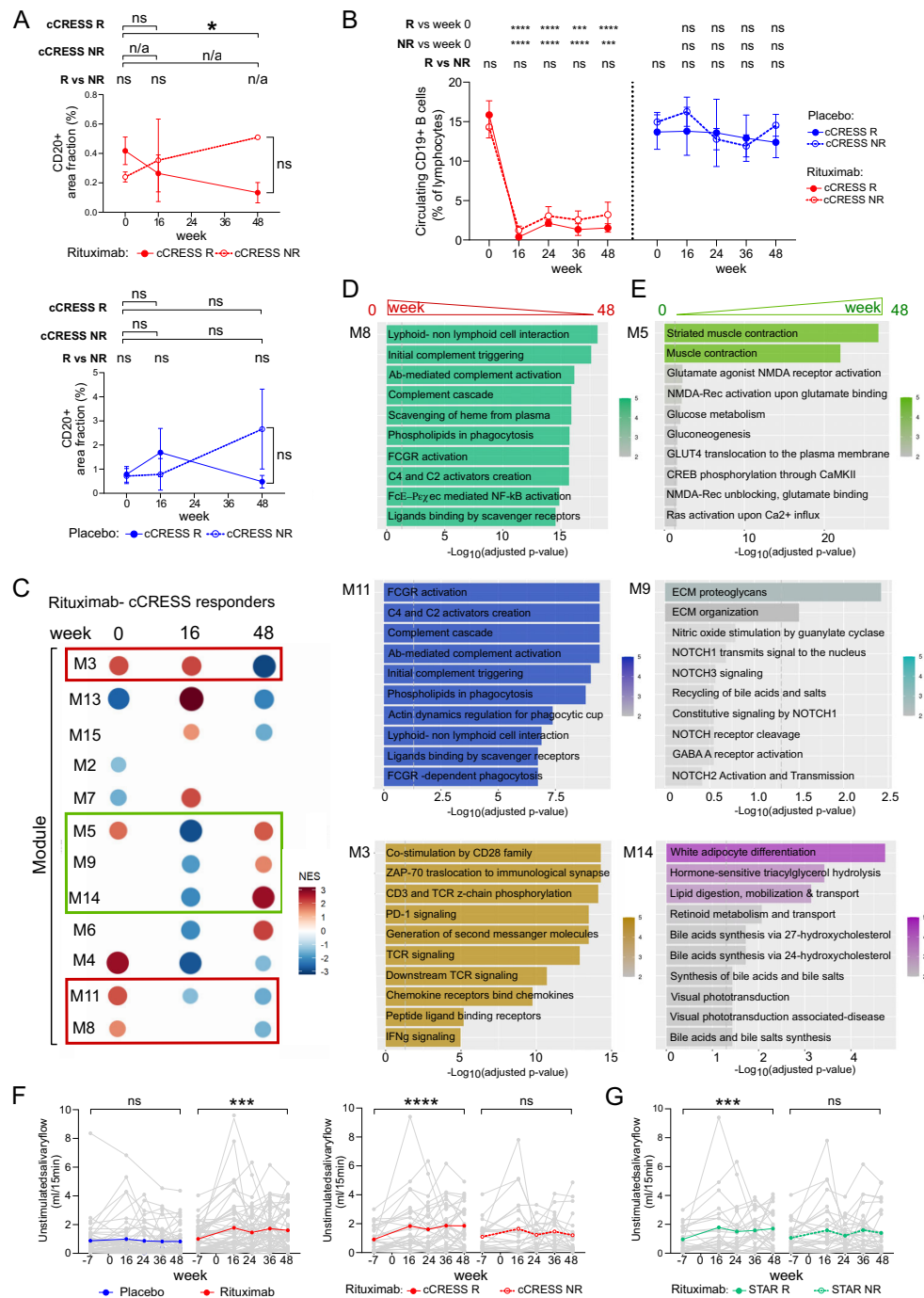


Figure 5. Histologic and transcriptomic changes associated to treatment response. Longitudinal changes in (A) LSG B cell area fraction and circulating B cells (B) in the rituximab and placebo groups, segregated according to cCRESS response. Data from patients who received placebo ($n = 12$) and rituximab ($n = 8$) are shown. Statistical analysis by Wilcoxon's rank sum test within groups was performed (top square brackets). Mann-Whitney U test between patients classified as responders or non responders was performed. The statistic for the week:treatment ratio interaction model on side square brackets is shown. ns $P \geq 0.05$, * $P < 0.05$, *** $P < 0.001$, **** $P < 0.0001$. (C) Heatmap of gene modules changes over time (weeks 0, 16, and 48) in rituximab cCRESS-responders patients. Pathway enrichment analysis of modules (modules 3, 8, and 11) (D) down-regulated and (E) up-regulated (modules 5, 9, and 14) from week 0 to week 48 in rituximab cCRESS-responders patients. The vertical dashed grey line indicates adjusted $P = 0.01$. Data are shown from patients who received rituximab ($n = 6$). Data from the LSG biopsies of patients who received rituximab ($n = 6$) are shown. Unstimulated salivary flow changes over time in (F) the group that received placebo ($n = 66$) and rituximab ($n = 66$), and within patients who received rituximab ($n = 66$), segregated according to (F) cCRESS and (G) STAR response. ns $P \geq 0.05$, * $P < 0.05$, *** $P < 0.001$, **** $P < 0.0001$. CaMK, Ca^{2+} /calmodulin-dependent protein kinase; cCRESS, concise Composite of Relevant Endpoints for Sjögren Syndrome; ECM, extra cellular matrix; FCGR, Fc γ receptor; GABA, γ -aminobutyric acid; GLUT, glucose transporter; IFN, interferon; n/a, not available; NES, normalized enrichment score; NMDA, N-methyl-D-aspartate; ns, not significant; PD, programmed cell death; Ras, rat sarcoma; Rec, receptor; TCR, T cell Receptor. Color figure can be viewed in the online issue, which is available at <http://onlinelibrary.wiley.com/doi/10.1002/art.42772/abstract>.

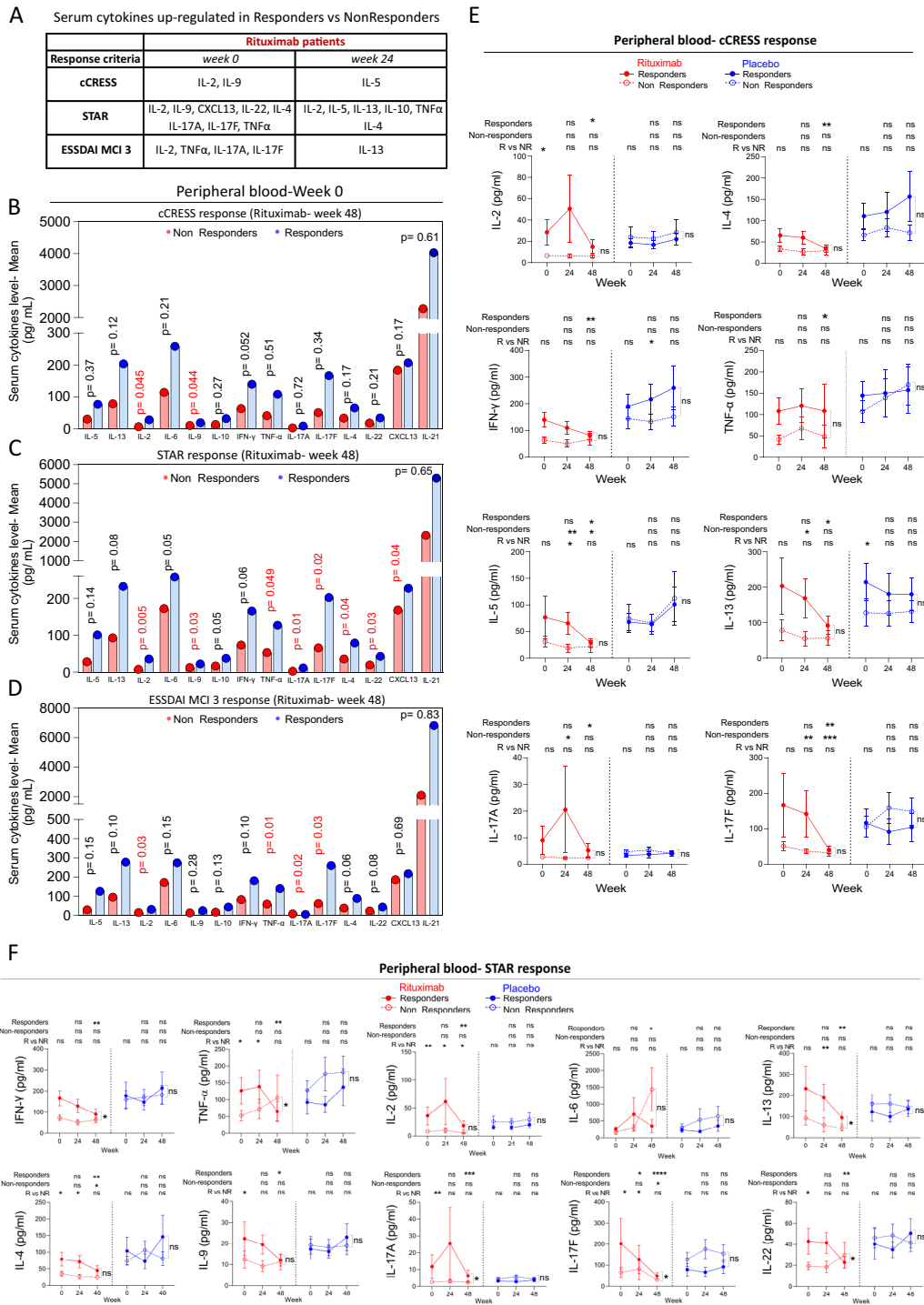


Figure 6. Serum and tissue biomarkers associated with treatment response. (A) Table summarizing the cytokine serum level up-regulated in patients who received rituximab ($n = 60$) classified as responders according to ESSDAI improvement, cCRESS, and STAR scores. (B–D) Comparison of mean value of cytokines levels in serum between responder and non-responder patients according to the ESSDAI improvement, cCRESS, and STAR scores. Mann–Whitney U test was used between responder and non-responder groups for each cytokine. Longitudinal analysis of cytokines level according to (E) cCRESS and (F) STAR response criteria. Mean \pm SEM values are shown. Statistical analysis by Wilcoxon’s rank sum test within groups is shown (top square brackets). Mann–Whitney U test was used between responder and non-responder patients at each time point. The statistic for the week:treatment ratio interaction model on side square brackets. Data from patients who received placebo ($n = 55$) and rituximab ($n = 54$) are shown. ns $P \geq 0.05$, * $P < 0.05$, ** $P < 0.01$, *** $P < 0.0001$. cCRESS, concise Composite of Relevant Endpoints for Sjögren Syndrome; CXCL, C-X-C motif chemokine ligand; ESSDAI, EULAR Sjögren Syndrome Disease Activity Index; IFN, interferon; IL, interleukin; MCI, minimal clinical improvement; ns, not significant; STAR, Sjögren Tool for Assessing Response; TNF, tumor necrosis factor. Color figure can be viewed in the online issue, which is available at <http://onlinelibrary.wiley.com/doi/10.1002/art.42772/abstract>.

DISCUSSION

Consensus on the efficacy of rituximab treatment in patients with pSS has been lacking, primarily because of two previous large RCTs—TEARS and TRACTISS—that failed to meet their primary endpoints. TEARS and TRACTISS were conducted before the use of ESSDAI as inclusion or response criteria. However, the recent reanalysis of TRACTISS and TEARS using the novel composite endpoints cCRESS and candidate STAR^{10,11} demonstrated a significantly higher response rate in patients who received rituximab versus those who received placebo in both studies. These novel observations reconcile with the observed improvement in biologic and histologic parameters previously reported in smaller studies (reviewed in Grigoriadou et al and Verstappen et al).^{7,23}

Here, we took advantage of the unique characteristics of the TRACTISS cohort in which blood and SG biopsies matched were collected over three time points (baseline and at 16 and 48 weeks), allowing an in-depth analysis of longitudinal changes in peripheral biomarkers, SG inflammation, and their relevance to clinical response. In particular, compared to previous studies evaluating peripheral blood and/or SG histology, at the study endpoint and over a shorter follow-up in smaller cohorts,^{7,23} the TRACTISS evaluates the ability of rituximab to improve/prevent evolution in SG immunopathology and systemic inflammation compared to its natural disease evolution in patients with pSS who received placebo. The combination of in-depth SG immunophenotyping linked with RNA-seq transcriptomic profiling unravels key mechanisms by which two cycles of rituximab resulted in the improvement or prevention of further progression of SG inflammation associated with amelioration or stabilization of exocrine gland function in the TRACTISS cohort over the 48 weeks of treatment. These results were in line with the previously reported improvement of unstimulated salivary flow⁹ and SG total US score¹³ in the TRACTISS cohort, confirming the importance of US as a sensitive surrogate of SG immunopathology in our cohort. Of note, baseline total US score positively correlated with the foci area in line with previous observations.²⁴

Differently from a previous study that identified higher baseline median B cell numbers in the parotid glands of patients who responded to rituximab,^{25,26} we could not identify any baseline SG predictors of disease response to rituximab in the TRACTISS trial. However, the combined baseline analysis of such a data-rich cohort highlighted several interesting correlations between SG immunopathology and parameters of B cell activation, including circulating IgG, IgM, and RF, the latter being an independent predictor of SG lymphoma progression.²⁷ The analysis of repeated SG biopsies, using traditional histopathology with digital image analysis quantitative assessment, showed that the focus score was unchanged over time in comparison to patients who received placebo. Treatment with rituximab prevented the enlargement of

SG aggregates measured as aggregate area fraction and mean aggregate size, confirming that these assessments are significantly more reliable and sensitive to change, compared to the traditional focus score.¹⁵

The first key novel observation in the longitudinal assessment of SG immunopathology in patients who received placebo is that the organization of inflammatory aggregates evolved over the 48 weeks of the study. In particular, further recruitment of B cells into the SG with higher degrees of lymphoid organization of ectopic GCs could be observed over 48 weeks in the placebo arm, associated with the increase in transcriptomic signatures critical for B and T cell recruitment, activation, and costimulation, which was efficiently prevented by rituximab. These findings are in line with the existing evidence that rituximab reduces the total number of SG-infiltrating B cells, both in LSGs^{28–31} and parotid SGs,^{32,33} despite the different rituximab dosage and administration regimen. This observation should prompt a rethinking of the notion that SG immunopathology is stable over time³⁴ and focus the longitudinal assessment of SGs in clinical trials both in terms of amelioration from baseline but also lack of progression.

Of relevance, a significant difference in the evolution of B cell infiltration over time was only observed in clinical responders patients, defined according to the novel composite endpoints criteria,^{10,11} suggesting that amelioration of SG immunopathology is a sensitive biomarker of clinical response when using composite endpoints that include objective assessment of exocrine function. The lack of new B cell migration within the SG after rituximab is possibly driven by the down-regulation of B lymphocyte chemoattractant chemokine CXCL13, observed in both circulation and within the SG tissue of patients who received rituximab. Over-expression of lymphoid chemokine CXCL13 and, to a lesser degree, CXCL12 lymphoid chemokines within SGs in patients with pSS exerts a critical role during ectopic lymphoid formation.³⁵

To what extent rituximab is able to target B cells within the SGs and whether preferential B cell subpopulations are preferentially targeted remains rather elusive. Here, using gene signature-based deconvolution tools applied to SG RNA-seq data, we identified preferential targeting of the memory compartment, in particular, switched memory B cells. Of note, the histologic and transcriptomic changes within LSG biopsies occurred only after the second cycle of rituximab, suggesting that a more prolonged depletion of circulating B cells may be required to observe significant changes in the SG persisting 6 months after rituximab was last received.

We observed longitudinal changes in T cell subsets infiltrating the SG, again showing opposing trends in patients who received rituximab versus those who received placebo. It was particularly interesting to observe the down-regulation of gene signatures specific to T cell subsets functionally related to GC formation and extrafollicular B cell activation, including T follicular

helper and T peripheral helper, which have been shown to be expanded in both the peripheral blood^{36,37} and SGs of patients with pSS.^{38,39}

The profound changes observed in SG immunopathology after receiving rituximab were mirrored by the clear evidence of the re-established expression of molecular pathways indicative of functional and metabolic restoration of the glandular epithelium. This pattern was observed in patients who were clinically responders to cCRESS, showing a preservation and/or improvement in the exocrine function, with similar observations for candidateSTAR responders.

These data provide a mechanistic explanation for the overall amelioration of UWSF in the group that received rituximab compared to placebo over 48 weeks, previously reported in the TRACTISS trial,⁹ and further support preliminary findings in parotid glands.⁴⁰ Furthermore, our data suggest that this process is related to both improvements in the SG histopathology in rituximab responders patients combined with the prevention of disease progression, observed in the placebo group.

Peripheral profiling of inflammatory cytokines involved in T and B cell responses at baseline identified several biomarkers associated with clinical response to rituximab according to STAR, but not cCRESS, criteria. These results suggest that (i) systemic evidence of immune activation is a prerequisite for clinical response to rituximab in some patients with SS, and (ii) STAR, which gives larger weight to ESSDAI compared to the ocular and oral response items (equally weighted in CRESS), captures changes in systemic disease in our trial. In keeping with the observation of a higher clinical response rates in immunologically active patients at baseline, receiving rituximab induced a longitudinal reduction of peripheral cytokines selectively in patients who responded to STAR criteria and, to lesser extent, cCRESS criteria, confirming that clinical response in a subset of patients is associated with the normalization of systemic inflammation.

In summary, the present work highlighted that rituximab can profoundly impact the underlying disease process, reducing peripheral immune activation and SG inflammation when received as repeated infusions and for a longer schedule compared to the majority of previously conducted clinical trials. These effects over placebo are related both to the improvement of SG immunopathology and the prevention of further evolution of local disease in untreated patients. Remarkably, the observed differences in cellular and molecular pathology over time are associated with clinical improvement assessed using novel composite endpoints such as cCRESS¹⁰ and candidate STAR,¹¹ which include objective measurement of exocrine function together with systemic disease and are currently being validated as primary endpoints for future clinical trials. Although the TRACTISS has provided the largest and most accurate longitudinal SG sample collection with linked cellular and molecular pathology data reported so far, it represents a relatively small cohort compared to randomized clinical trials conducted in other rheumatic conditions.^{41,42} As such, the

novel cellular and molecular pathology biomarkers reported in this study will require further validation. Such work is currently being implemented as part of the IMI2-NECESSITY consortium (<https://www.imi.europa.eu/projects-results/project-factsheets/necessity>), which will provide access to longitudinal labial and parotid biopsies from recently completed clinical trials, including ones in which patients received abatacept⁴³ and a most recent trial in which patients received rituximab in combination with anti-BAFF monoclonal antibody (belimumab).^{44,45}

ACKNOWLEDGMENTS

We thank the National Institute for Health Research Leeds Clinical Trial Unit, which coordinated the trial.

AUTHOR CONTRIBUTIONS

All authors were involved in drafting the article or revising it critically for important intellectual content, and all authors approved the final version to be published. Drs. Pontarini and Bombardieri had full access to all of the data in the study and take responsibility for the integrity of the data and the accuracy of the data analysis.

Study conception and design. Pontarini.

Acquisition of data. Pontarini, Chowdhury, Grigoriadou, Murray-Brown, Luchessi, Jaworska, Ghirardi, Emery, Ng, Sutcliffe, Tappuni, Cavallaro.

Analysis and interpretation of data. Pontarini, Sciacca, Chowdhury, Grigoriadou, Rivellesse, Murray-Brown, Lucchesi, Fossati-Jimack, Nerviani, Giacomassi, Emery, Ng, Everett, Fernandez, Seror, Mariette, Porcher, Cavallaro, Pulvirenti, Verstappen, de Wolff, Arends, Bootsma, Lewis, Pitzalis, Bowman, Bombardieri.

REFERENCES

1. Brito-Zerón P, Baldini C, Bootsma H, et al. Sjögren syndrome. *Nat Rev Dis Prim* 2016;2:16047.
2. Saraux A, Pers JO, Devauchelle-Pensec V. Treatment of primary Sjögren syndrome. *Nat Rev Rheumatol* 2016;12:456–471.
3. Hansen A, Odendahl M, Reiter K, et al. Diminished peripheral blood memory B cells and accumulation of memory B cells in the salivary glands of patients with Sjögren's syndrome. *Arthritis Rheum* 2002;46:2160–2171.
4. Hansen A, Reiter K, Ziprian T, et al. Dysregulation of chemokine receptor expression and function by B cells of patients with primary Sjögren's syndrome. *Arthritis Rheum* 2005;52:2109–2119.
5. Christodoulou MI, Kapsogeorgou EK, Moutsopoulos HM. Characteristics of the minor salivary gland infiltrates in Sjögren's syndrome. *J Autoimmun* 2010;34:400–407.
6. Nocturne G, Pontarini E, Bombardieri M, et al. Lymphomas complicating primary Sjögren's syndrome: from autoimmunity to lymphoma. *Rheumatology* 2021;60:3513–3521.
7. Grigoriadou S, Chowdhury F, Pontarini E, et al. B cell depletion with rituximab in the treatment of primary Sjögren's syndrome: what have we learnt? *Clin Exp Rheumatol* 2019;37(Suppl 1):217–224.
8. Devauchelle-Pensec V, Mariette X, Jousse-Joulin S, et al. Treatment of primary Sjögren syndrome with rituximab. *Ann Intern Med* 2014;160:233–242.
9. Bowman SJ, Everett CC, O'Dwyer JL, et al. Randomized controlled trial of rituximab and cost-effectiveness analysis in treating fatigue and oral dryness in primary Sjögren's syndrome. *Arthritis Rheumatol* 2017;69:1440–1450.

10. Arends S, de Wolff L, van Nimwegen JF, et al. Composite of Relevant Endpoints for Sjögren's Syndrome (CRESS): development and validation of a novel outcome measure. *Lancet Rheumatol* 2021;3:e553–e562.
11. Seror R, Baron G, Camus M, et al. Development and preliminary validation of the Sjögren's Tool for Assessing Response (STAR): a consensual composite score for assessing treatment effect in primary Sjögren's syndrome. *Ann Rheum Dis* 2022;81:979–989.
12. Brown S, Navarro Coy N, Pitzalis C, et al. The TRACTISS protocol: a randomised double blind placebo controlled clinical TRial of Anti-B-Cell Therapy In patients with primary Sjögren's Syndrome. *BMC Musculoskelet Disord* 2014;15:21.
13. Fisher BA, Everett CC, Rout J, et al. Effect of rituximab on a salivary gland ultrasound score in primary Sjögren's syndrome: results of the TRACTISS randomised double-blind multicentre substudy. *Ann Rheum Dis* 2018;77:412–416.
14. Bankhead P, Loughrey MB, Fernández JA, et al. QuPath: open source software for digital pathology image analysis. *Sci Rep* 2017;7:16878.
15. Lucchesi D, Pontarini E, Donati V, et al. The use of digital image analysis in the histological assessment of Sjögren's syndrome salivary glands improves inter-rater agreement and facilitates multicentre data harmonisation. *Clin Exp Rheumatol* 2021;38(Suppl 1):180–188.
16. Fisher BA, Jonsson R, Daniels T, et al. Standardisation of labial salivary gland histopathology in clinical trials in primary Sjögren's syndrome. *Ann Rheum Dis* 2017;76:1161–1168.
17. Sturm G, Finotello F, Petitprez F, et al. Comprehensive evaluation of transcriptome-based cell-type quantification methods for immunocytology. *Bioinformatics* 2019;35:i436–i445.
18. Aran D, Hu Z, Butte AJ. xCell: digitally portraying the tissue cellular heterogeneity landscape. *Genome Biol* 2017;18:220.
19. Zhang F, Wei K, Slowikowski K, et al. Defining inflammatory cell states in rheumatoid arthritis joint synovial tissues by integrating single-cell transcriptomics and mass cytometry. *Nat Immunol* 2019;20:928–942.
20. Russo PST, Ferreira GR, Cardozo LE, et al. CEMiTool: a Bioconductor package for performing comprehensive modular co-expression analyses. *BMC Bioinformatics* 2018;19:56.
21. Cheng CW, Beech DJ, Wheatcroft SB. Advantages of CEMiTool for gene co-expression analysis of RNA-seq data. *Comput Biol Med* 2020;125:103975.
22. Metzler MA, Raja S, Elliott KH, et al. RDH10-mediated retinol metabolism and RAR α -mediated retinoic acid signaling are required for submandibular salivary gland initiation. *Development* 2018;145:dev164822.
23. Verstappen GM, van Nimwegen JF, Vissink A, et al. The value of rituximab treatment in primary Sjögren's syndrome. *Clin Immunol* 2017;182:62–71.
24. Baldini C, Luciano N, Tarantini G, et al. Salivary gland ultrasonography: a highly specific tool for the early diagnosis of primary Sjögren's syndrome. *Arthritis Res Ther* 2015;17:146.
25. Cornec D, Costa S, Devauchelle-Pensec V, et al. Do high numbers of salivary gland-infiltrating B cells predict better or worse outcomes after rituximab in patients with primary Sjögren's syndrome? *Ann Rheum Dis* 2016;75:e33.
26. Delli K, Haacke EA, Kroese FGM, et al. In primary Sjögren's syndrome high absolute numbers and proportions of B cells in parotid glands predict responsiveness to rituximab as defined by ESSDAI, but not by SSRI. *Ann Rheum Dis* 2016;75:e34.
27. Nocturne G, Virone A, Ng WF, et al. Rheumatoid factor and disease activity are independent predictors of lymphoma in primary Sjögren's syndrome. *Arthritis Rheumatol* 2016;68:977–985.
28. Devauchelle-Pensec V, Pennec Y, Morvan J, et al. Improvement of Sjögren's syndrome after two infusions of rituximab (anti-CD20). *Arthritis Rheum* 2007;57:310–317.
29. Pers JO, Devauchelle V, Daridon C, et al. BAFF-modulated repopulation of B lymphocytes in the blood and salivary glands of rituximab-treated patients with Sjögren's syndrome. *Arthritis Rheum* 2007;56:1464–1477.
30. Carubbi F, Cipriani P, Marrelli A, et al. Efficacy and safety of rituximab treatment in early primary Sjögren's syndrome: a prospective, multicenter, follow-up study. *Arthritis Res Ther* 2013;15:R172.
31. Cornec D, Costa S, Devauchelle-Pensec V, et al. Blood and salivary-gland BAFF-driven B-cell hyperactivity is associated to rituximab inefficacy in primary Sjögren's syndrome. *J Autoimmun* 2016;67:102–110.
32. Pijpe J, Meijer JM, Bootsma H, et al. Clinical and histologic evidence of salivary gland restoration supports the efficacy of rituximab treatment in Sjögren's syndrome. *Arthritis Rheum* 2009;60:3251–3256.
33. Delli K, Haacke EA, Kroese FGM, et al. Towards personalised treatment in primary Sjögren's syndrome: baseline parotid histopathology predicts responsiveness to rituximab treatment. *Ann Rheum Dis* 2016;75:1933–1938.
34. Kapsogeorgou EK, Christodoulou MI, Panagiotakos DB, et al. Minor salivary gland inflammatory lesions in Sjögren syndrome: do they evolve? *J Rheumatol* 2013;40:1566–1571.
35. Hansen A, Lipsky PE, Dörner T. B cells in Sjögren's syndrome: indications for disturbed selection and differentiation in ectopic lymphoid tissue. *Arthritis Res Ther* 2007;9:218.
36. Dupré A, Pascaud J, Rivière E, et al. Association between T follicular helper cells and T peripheral helper cells with B-cell biomarkers and disease activity in primary Sjögren syndrome. *RMD Open* 2021;7:e001442.
37. Verstappen GM, Meiners PM, Corneth OBJ, et al. Attenuation of follicular helper T cell-dependent B cell hyperactivity by abatacept treatment in primary Sjögren's syndrome. *Arthritis Rheumatol* 2017;69:1850–1861.
38. Pontarini E, Murray-Brown WJ, Croia C, et al. Unique expansion of IL-21+ Tfh and Tph cells under control of ICOS identifies Sjögren's syndrome with ectopic germinal centres and MALT lymphoma. *Ann Rheum Dis* 2020;79:1588–1599.
39. Fonseca VR, Romão VC, Agua-Doce A, et al. The ratio of blood T follicular regulatory cells to T follicular helper cells marks ectopic lymphoid structure formation while activated follicular helper T cells indicate disease activity in primary Sjögren's syndrome. *Arthritis Rheumatol* 2018;70:774–784.
40. Pijpe J, Meijer JM, Bootsma H, et al. Clinical and histologic evidence of salivary gland restoration supports the efficacy of rituximab treatment in Sjögren's syndrome. *Arthritis Rheum* 2009;60:3251–3256.
41. Humby F, Durez P, Buch MH, et al. Rituximab versus tocilizumab in anti-TNF inadequate responder patients with rheumatoid arthritis (R4RA): 16-week outcomes of a stratified, biopsy-driven, multicentre, open-label, phase 4 randomised controlled trial. *Lancet* 2021;397:305–317.
42. Rivellese F, Surace AE, Goldmann K, et al. Rituximab versus tocilizumab in rheumatoid arthritis: synovial biopsy-based biomarker analysis of the phase 4 R4RA randomized trial. *Nat Med* 2022;28:1256–1268.
43. van Nimwegen JF, Mossel E, van Zuiden GS, et al. Abatacept treatment for patients with early active primary Sjögren's syndrome: a single-centre, randomised, double-blind, placebo-controlled, phase 3 trial (ASAP-III study). *Lancet Rheumatol* 2020;2:e153–e163.
44. Mariette X, Baldini C, Barone F, et al. OP0135 safety and efficacy of subcutaneous belimumab and intravenous rituximab combination in patients with primary Sjögren's syndrome: a phase 2, randomised, placebo-controlled 68-week study. *Ann Rheum Dis* 2021;80:78.2–79.
45. Bootsma H, Arends S, de Wolff L, et al. POS0193 evaluation of CRESS in the phase 2 randomised placebo-controlled study of sequential belimumab/rituximab administration in patients with primary Sjögren's syndrome. *Ann Rheum Dis* 2022;81:329.1–330.